Modeling and simulation of the diffusive transport in a nanoscale Double-Gate MOSFET

P. Pietra[a], N. Vauchelet[b,1]

[a] Istituto di Matematica Applicata e Tecnologie Informatiche, C.N.R.,
Via Ferrata 1, 27100 Pavia, Italy
[b] Institut de Mathématiques de Toulouse, (UMR 5219), Université Paul Sabatier,
118, route de Narbonne, 31062 Toulouse cedex 4, France

E-mail addresses: paola.pietra@imati.cnr.it ; vauchel@mip.ups-tlse.fr.

Abstract

In this work we present the mathematical modeling and the simulation of the diffusive transport of an electron gas confined in a nanostructure. A coupled quantum-classical system is considered, where the coupling occurs in the momentum variable : the electrons are like point particles in the direction parallel to the gas, while they behave like waves in the transverse direction. A drift-diffusion description in the transport direction is obtained thanks to an asymptotic limit of the Boltzmann transport equation for confined electrons. The system is used to model the transport of charged carriers in a nanoscale Double-Gate MOSFET. Simulations of transport in such a device are presented.

Keywords : Schrödinger equation, Drift-Diffusion system, Subband model, Nanotransistor, Gummel iterations.

1 Introduction

The significant trend of miniaturization in Microelectronics brougth, in the recent years, the scaling process down to the nanometer scale, with improvements in speed and functionality of electronic components. In this task, modeling and numerical simulation play an important role to predict the behaviour of devices whose electron transport properties are largely based on quantum effects [1, 2, 3]. In these ultimate size devices like nanoscale Double-Gate MOSFETs [4], electrons might be extremely confined in one or several directions, which are referred to as the confined directions. This leads to a partial quantization of energies. This article proposes to describe nanoscale semiconductor devices using a subband decomposition approach which consists of a diagonalization of the Hamiltonian on slices perpendicular to the transport direction. A self-consistent process between the calculation of the electron density and the space charge effects using the Poisson equation is defined. The subband model describes the system as a statistical mixture of eigenstates of the Schrödinger operator in the confined direction. The elementary states are obtained thanks to the resolution of a classical transport equation. Thanks to the separation

[1] *Corresponding author.*

of the confined and the transport directions, the computational gain is significant by the reduction of the dimension of the transport problem [5, 6].

Here, we consider a diffusive transport described by means of a drift–diffusion model [7, 8, 9]. Starting from a set of Boltzmann equations, one for each subband, we derive the effective potential energy for the single drift–diffusion equation of the model. Under the assumption of dominant electron–phonon scattering, which is the leading scattering mechanism in the diffusive regime, a limit in the scaled mean free path is performed. The main difficulty here stands in the highly non linear coupling with the subband decomposition method. Though for devices with short channel length far-from-equilibrium effects become relevant (see [10, 11], e.g.) and higher order moment models seem to be more appropriate, however the low computational cost and the good convergence properties of the iteration procedure make attractive the use of a drift–diffusion model for rapid design calculation. The simulation results presented in Section 5 show a good agreement with similar results reported in the literature and obtained with Monte–Carlo simulation [12].

In ultra short channel devices quantum effects (such as tunneling from source to drain) take place in the transport direction and classical transport cannot be used. We refer to [13, 5], where a purely ballistic quantum transport of Schrödinger type and its numerical treatment relying on the subband approach are presented.

In the recent literature, wide interest has been shown in modifications of the drift–diffusion model (of low computational cost) in order to take into account quantum effects, see e.g. [14, 15, 16]. A full quantum drift-diffusion model (quantum in both directions) was derived in [17] and its numerical simulation was addressed in [18]. A quite similar model was introduced in [19] and used in [20] to simulate nanoscale MOSFETs. A quantum drift-diffusion model is presented and simulated as a nonlinear parabolic system in [21], in order to describe the switching behavior of a resonant tunneling diode.

The paper is organized as follows. In Section 2 we present an overview of the model under consideration. Section 3 deals with the formal diffusive limit of the Boltzmann semiconductor equation towards the drift-diffusion equation. Moreover, modifications in the model when anisotropy of silicon is taken into account are introduced. In Section 4 we describe the numerical scheme and the iterative procedure used in the simulation. Finally, results of the simulation of a nanoscale Double-Gate MOSFET are presented in the last section.

2 Presentation of the model

In this section we present the model used and implemented in this work. We assume to have one confined direction, that we denote by z, belonging to the interval $[0, \ell]$. The transport direction(s) are denoted by x.

2.1 The subband decomposition method

In the subband decomposition approach the system is viewed as a statistical mixture of eigenstates of the Schrödinger operator in the confined direction. The occupation number of each state is given by a statistic function: for Boltzmann statistics it is $\exp(\frac{\epsilon_F-\epsilon}{k_BT_L})$, for Fermi-Dirac statistics this is $1/(1+\exp(\frac{\epsilon-\epsilon_F}{k_BT_L}))$. In these expressions ϵ is the energy of the considered state, k_B is the Boltzmann constant, T_L is the lattice temperature and ϵ_F is the so-called Fermi energy which, at zero temperature, represents the threshold between occupied and unoccupied states [22, 23, 24].

In the confined direction, the system is assumed to be at equilibrium with a local Fermi level ϵ_F which depends on the transport variable x. At a position (x, z), the particle density $N(x, z)$ for Boltzmann statistics is given by

$$N(x,z) = \sum_{k=1}^{+\infty} e^{\beta(\epsilon_F(x)-\epsilon_k(x))}|\chi_k(x,z)|^2, \tag{1}$$

where $\beta = 1/(k_BT_L)$ and $(\chi_k, \epsilon_k)_{k\geq 1}$ is the complete set of eigenfunctions and eigenvalues of the Schrödinger operator in the z variable

$$\begin{cases} -\dfrac{\hbar^2}{2}\dfrac{d}{dz}\left(\dfrac{1}{m^*(z)}\dfrac{d}{dz}\chi_k\right) + U\chi_k = \epsilon_k\chi_k, \\ \chi_k(x,\cdot) \in H_0^1(0,\ell), \quad \displaystyle\int_0^\ell \chi_k\,\chi_{k'}\,dz = \delta_{kk'}\,. \end{cases} \tag{2}$$

In this equation $\hbar$ is the reduced Planck constant, m^* the effective mass. Moreover, U is the potential energy defined by $U = -eV$, where e the elementary charge and V denotes the self-consistent electrostatic potential, solution of the Poisson equation

$$\text{div}_{x,z}(\varepsilon_R(x,z)\nabla_{x,z}V) = \frac{e}{\varepsilon_0}(N - N_D). \tag{3}$$

Here $\varepsilon_R(x, z)$ denotes the relative permittivity, ε_0 the permittivity constant in vacuum and $N_D(x, z)$ is the prescribed doping density.

2.2 The diffusive regime

In the transport direction(s), we consider a purely classical transport in the diffusive regime, which is described by the stationary drift-diffusion equation :

$$-\text{div}_x\, J(x) = 0, \tag{4}$$

$$J(x) = \mathbb{D}(\nabla_x N_s(x) + \beta N_s(x)\nabla_x U_s(x)), \tag{5}$$

where N_s is the surface density, $\mathbb{D}$ denotes the diffusion coefficient $\mathbb{D} = \mu k_BT_L$ for a constant mobility μ and the effective energy U_s is given by

$$U_s = -k_BT_L \log\left(\sum_{k=1}^{+\infty} e^{-\beta\epsilon_k}\right). \tag{6}$$

If we define the repartition function $\mathcal{Z}$ as

$$\mathcal{Z}(x) = \sum_{k=1}^{+\infty} e^{-\beta\epsilon_k(x)}, \tag{7}$$

then, we obtain easily from (1) and (2) that the surface density satisfies

$$N_s(x) = \int_0^\ell N(x,z)\,dz = e^{\beta\epsilon_F}\mathcal{Z}(x).$$

Therefore, $\epsilon_F(x)$ in (1) can be written in terms of N_s and N_s can be chosen as unknown in the model. We have then

$$N(x,z) = \frac{N_s(x)}{\mathcal{Z}(x)} \sum_{k=1}^{+\infty} e^{-\beta\epsilon_k(x)} |\chi_k(x,z)|^2. \tag{8}$$

If we introduce the Slotboom variable u defined by

$$u(x) = e^{\beta\epsilon_F} = \frac{N_s(x)}{\mathcal{Z}(x)}, \tag{9}$$

then, we get easily that the drift-diffusion equation (4)–(5) reads

$$-\text{div}_{\,x}(\mathbb{D}\mathcal{Z}(x)\nabla_x u(x)) = 0. \tag{10}$$

The drift-diffusion equation can be derived from kinetic theory when the mean free path is small compared to the system length-scale [25, 26]. Such a derivation from the semiconductor Boltzmann equation is formally derived in Section 3.

The unknowns of the overall system are the surface density $N_s(x)$, the eigenenergies $\epsilon_k(x)$, the eigenfunctions $\chi_k(x,z)$ and the electrostatic potential $V(x,z)$. If we assume that the electrostatic potential V is given, then a diagonalization of the one dimensional Schrödinger operator (2) provides the eigenvalues and eigenvectors (ϵ_k, χ_k). The effective energy U_s can be computed from (6). This allows us to obtain the surface density N_s by solving the drift-diffusion problem (4)–(5). Then, the density N is evaluated using (8) and a new potential is computed by solving Poisson equation (3).

This fix point map is used in [27] to establish existence of solutions. More details about its use as numerical algorithm are given in Section 4.

3 Formal limit of the Boltzmann equation to the drift-diffusion equation

In order to understand the expression of the effective energy U_s given in (6) and the role of the effective mass when the anisotropy of silicon is taken into account, we present in this section the formal derivation of the stationary drift-diffusion equation

from the semiconductor Boltzmann equation for the subband model. The diffusive limit of the Boltzmann equation towards the drift-diffusion equation is well known (see [25, 26] for a rigorous proof of this limit). In the subband decomposition approach, because of the non linear coupling with the Schrödinger-Poisson system, we need to renormalize the Boltzmann equation. We refer to [28] for the rigorous derivation.

Let $\eta > 0$ be the scaled mean free path assumed to be small. We consider the scaled Boltzmann equation for the subband model defined on the phase space $\mathbb{R}^2 \times \mathbb{R}^2$. We denote by x the position, $x \in \mathbb{R}^2$, and by p the momentum, $p \in \mathbb{R}^2$. The time variable t is nonnegative. We consider a diffusion scaling with parameter η

$$t' = \eta^2 t \text{ and } x' = \eta x.$$

Then, (writing again t for t' and x for x') the electron distribution function in each subband f_k^η satisfies (see [26] and references therein)

$$\partial_t f_k^\eta + \frac{1}{\eta}(\frac{p}{m^*} \cdot \nabla_x f_k^\eta - \nabla_x \epsilon_k \cdot \nabla_p f_k^\eta) = \frac{1}{\eta^2} Q_B(f^\eta)_k, \tag{11}$$

which can be rewritten as

$$\partial_t f_k^\eta + \frac{1}{\eta}\{\mathcal{H}_k, f_k^\eta\} = \frac{1}{\eta^2} Q_B(f^\eta)_k,$$

where $\{\cdot,\cdot\}$ denotes the Poisson bracket : $\{g,h\} = \nabla_x h \cdot \nabla_p g - \nabla_p h \cdot \nabla_x g$. Moreover $\mathcal{H}_k$ is the energy of the system in the kth subband

$$\mathcal{H}_k(t,x,p) = \frac{1}{2}\frac{|p|^2}{m^*} + \epsilon_k(t,x).$$

The collision operator Q_B, describing the scattering between electrons and phonons, is assumed in the linear BGK approximation for Boltzmann statistics.

It reads in the following form :

$$Q_B(f)_k = \sum_{k'=1}^{+\infty} \int_{\mathbb{R}^2} \alpha_{k,k'}(p,p')(\mathcal{M}_k(p) f_{k'}(p') - \mathcal{M}_{k'}(p') f_k(p))\, dp', \tag{12}$$

where the function $\mathcal{M}_k$ is the Maxwellian

$$\mathcal{M}_k(t,x,p) = \frac{1}{2\pi m^* k_B T_L \mathcal{Z}(t,x)} e^{-\beta \mathcal{H}_k(t,x,p)}, \tag{13}$$

normalized such that

$$\sum_{k=1}^{+\infty} \int_{\mathbb{R}^2} \mathcal{M}_k dp = 1,$$

and where the repartition function $\mathcal{Z}$ is given by (7).

Here and in the following, we shall use the notation g_k for a function depending on the k-th subband, and the notation $g = (g_k)_{k\geq 1}$ when the entire set of subbands is taken into account.

Assumption 3.1 *The cross-section α is symmetric and bounded from above and from below:*

$$\exists\, \alpha_1, \alpha_2 > 0,\ 0 < \alpha_1 \leq \alpha_{k,k'}(p,p') \leq \alpha_2, \forall\, k, k' \geq 1,\ \forall\, p \in \mathbb{R}^2,\ \forall\, p' \in \mathbb{R}^2. \tag{14}$$

The initial condition is assumed to be given by :

$$f^\eta(0,x,p) = f^{in}(x,p). \tag{15}$$

For the sake of simplicity, we consider the transport on the whole space $\mathbb{R}^2$ with no charge carriers at infinity : $\lim_{|x|\to+\infty} f(t,x,p) = 0$.

Assumption 3.2 *We assume that the given initial condition satisfies $f^{in} \in \ell^1(L^\infty(\mathbb{R}^2 \times \mathbb{R}^2))$, $f^{in} \geq 0$.*

Assumption 3.3 *We assume that the potential energy ϵ_k is given for all $k \geq 1$ in $L^\infty((0,T), H^1(\mathbb{R}^2))$ and that $\partial_t \epsilon_k \in L^\infty((0,T)\times\mathbb{R}^2)$, that is*

$$\exists\, \mu > 0 \text{ such that } \forall\, (t,x) \in (0,T)\times\mathbb{R}^2,\ |\partial_t \epsilon_k| \leq \mu. \tag{16}$$

Moreover, we suppose that $(\epsilon_k)_{k\geq 1}$ is a nondecreasing sequence of positive functions satisfying

$$\exists\, C > 0,\ \forall\, (t,x) \in (0,T)\times\mathbb{R}^2,\ \forall\, k \geq 1,\ |\epsilon_k(t,x) - \frac{1}{2}\pi^2 k^2| \leq C_0,$$

such that we can give a sense to $\mathcal{Z}$ in (7).

Remark 3.4 *Assumptions 3.3 are not really strong. Indeed, if ϵ_k is given by the subband model, i.e. it is the k-th eigenvalue of the stationary Schrödinger operator for an electrostatic potential energy U, then all these estimates hold true with constants μ and C_0 depending on U (see [29] and appendix of [27]). It remains to obtain some regularity on the potential energy U.*

3.1 Properties of the collision operator

In this section, the time variable t and the position x are only parameters, and, for the sake of simplicity, we omit the dependence on t and x and only consider the dependence on p. Here we establish some well-known properties of the collision operator Q_B defined by (12). To this aim, we define the weighted-space

$$L^2_{\mathcal{M}} = \{f = (f_k)_{k\geq 1} \text{ such that } \sum_{k=1}^{+\infty} \int_{\mathbb{R}^2} \frac{f_k^2}{\mathcal{M}_k}\, dp < \infty\}, \tag{17}$$

which is an Hilbert space with the scalar product

$$\langle f, g\rangle_{\mathcal{M}} = \sum_{k=1}^{+\infty} \int_{\mathbb{R}^2} \frac{f_k g_k}{\mathcal{M}_k}\, dp.$$

Proposition 3.5 *We assume that the cross-section α satisfies* (14). *Then the following properties hold for Q_B :*

(i) $\sum_k \int Q_B(f)_k \, dp = 0$.

(ii) *Q_B is a linear, selfadjoint and negative bounded operator on $L^2_{\mathcal{M}}$.*

(iii) *$Ker\, Q_B = \{f \in L^2_{\mathcal{M}}$, such that $\exists\, N_s \in \mathbb{R}, f_k = N_s \mathcal{M}_k\}$.*

(iv) *If $\mathcal{P}$ is the orthogonal projection on $Ker\, Q_B$ with the scalar product $\langle \cdot, \cdot \rangle_{\mathcal{M}}$, then*

$$-\langle Q_B(f), f \rangle_{\mathcal{M}} \geq \alpha_1 \| f - \mathcal{P}(f) \|^2_{\mathcal{M}}. \tag{18}$$

Proof. (i) follows immediately from the symmetry of the cross-section.
For the sake of simplicity we will use the standard notation $f' = f(p')$. For proving (ii), we start with writing:

$$\langle Q_B(f), g \rangle_{\mathcal{M}} = \sum_{k,k'} \int_{(\mathbb{R}^2)^2} \alpha_{k,k'} \mathcal{M}_k \mathcal{M}'_{k'} \left(\frac{f'_{k'}}{\mathcal{M}'_{k'}} - \frac{f_k}{\mathcal{M}_k} \right) \frac{g_k}{\mathcal{M}_k} \, dp dp'.$$

With our assumption (14) and the fact that $(\sum_k \int |f_k| \, dp)^2 \leq \|f\|^2_{\mathcal{M}}$ we get

$$|\langle Q_B(f), g \rangle_{\mathcal{M}}| \leq C \|f\|_{\mathcal{M}} \|g\|_{\mathcal{M}} \, ,$$

for all f, g in $L^2_{\mathcal{M}}$. Thus, Q_B is bounded. Moreover, we obtain easily

$$\langle Q_B(f), g \rangle_{\mathcal{M}} \ = -\frac{1}{2} \sum_{k,k'} \int_{(\mathbb{R}^2)^2} \alpha_{k,k'} \mathcal{M}_k \mathcal{M}'_{k'} \left(\frac{f'_{k'}}{\mathcal{M}'_{k'}} - \frac{f_k}{\mathcal{M}_k} \right) \left(\frac{g'_{k'}}{\mathcal{M}'_{k'}} - \frac{g_k}{\mathcal{M}_k} \right) dp dp'. \tag{19}$$

This provides the selfadjointness and negativity of Q_B.

The inclusion $\supseteq$ in (iii) is obvious. If $f \in Ker\, Q_B$, then $\langle Q_B(f), f \rangle_{\mathcal{M}} = 0$ and equality (19) implies that f_k coincide with the Maxwellian up to a multiplicative constant.Thus, (iii) holds true.

We are left with proving (iv). The definition of $L^2_{\mathcal{M}}$ and (iii) allow us to characterize $(Ker\, Q_B)^{\perp}$ as

$$(Ker\, Q_B)^{\perp} = \{ f \in L^2_{\mathcal{M}} \ \text{ such that } \ \sum_{k=1}^{+\infty} \int_{\mathbb{R}^2} f_k \, dp = 0 \}. \tag{20}$$

We have,

$$\begin{aligned} \langle Q_B(f), f \rangle_{\mathcal{M}} \ &= \langle Q_B(f) - Q_B(\mathcal{P}(f)), f \rangle_{\mathcal{M}} = \langle f - \mathcal{P}(f), Q_B(f) \rangle_{\mathcal{M}} \\ &= \langle g, Q_B(g) \rangle_{\mathcal{M}} \, , \end{aligned}$$

where we take $g = f - \mathcal{P}(f)$. Therefore, by using (19) we obtain

$$-\langle Q_B(f), f \rangle_{\mathcal{M}} = \frac{1}{2} \sum_{k,k'} \int_{(\mathbb{R}^2)^2} \alpha_{k,k'} \mathcal{M}_k \mathcal{M}'_{k'} \left(\frac{g'_{k'}}{\mathcal{M}'_{k'}} - \frac{g_k}{\mathcal{M}_k} \right)^2 dp dp'. \tag{21}$$

From (14) and since $g \in (Ker\, Q_B)^\perp$, (21) gives

$$-\langle Q_B(f), f\rangle_{\mathcal{M}} \geq \alpha_1 \sum_{k=1}^{+\infty} \left(\int_{\mathbb{R}^2} \frac{g_k^2}{\mathcal{M}_k}\, dp \right) \alpha_1 \|f - \mathcal{P}(f)\|_{\mathcal{M}}^2.$$

□

Proposition 3.6 *$Im\, Q_B$ is a closed subset of $L^2_{\mathcal{M}}$.*

Proof. Let $(h_n)_{n\in\mathbb{N}} \in Im\, Q_B$ be a sequence converging towards h in $L^2_{\mathcal{M}}$. Since $h_n = Q_B(f_n) = Q_B(g_n)$, where $g_n = f_n - P(f_n)$, Proposition 3.5 (ii) and (iv) imply

$$\alpha_1 \|g_n - g_m\|_{\mathcal{M}}^2 \leq \|h_n - h_m\|_{\mathcal{M}} \|g_n - g_m\|_{\mathcal{M}}.$$

This gives that (g_n) is a Cauchy sequence in $L^2_{\mathcal{M}}$. Thus, there exists $g \in L^2_{\mathcal{M}}$ such that $g_n \longrightarrow g$. By continuity of Q_B and uniqueness of the limit, $h = Q_B(g)$. □

Corollary 3.7 *Since Q_B is selfadjoint, we have $(Ker\, Q_B)^\perp = Im\, Q_B$.*
Thus $Q_B(f) = h$ admits a solution in $L^2_{\mathcal{M}}$ iff $h \in (Ker\, Q_B)^\perp$. Moreover this solution is unique if we impose $f \in (Ker\, Q_B)^\perp$.

Proposition 3.8 *There exists $\Theta \in (L^2_{\mathcal{M}})^2$ such that for all $k \geq 1$,*

$$Q_B(\Theta)_k = -\frac{p}{m^*}\mathcal{M}_k \quad \textit{and} \quad \sum_{k=1}^{+\infty} \int_{\mathbb{R}^2} \Theta_k\, dp = 0. \tag{22}$$

We define the diffusion matrix by

$$\mathbb{D} = \int_{\mathbb{R}^2} \sum_{k=1}^{+\infty} \Theta_k \otimes \frac{p}{m^*}\, dp. \tag{23}$$

Then, $\mathbb{D}$ is a symmetric coercive matrix.

Proof. (22) is an easy consequence of Corollary 3.7 and of (20). It remains to prove the symmetry and the coercivity of $\mathbb{D}$.

$$\mathbb{D}_{i,j} = \frac{1}{m^*} \int_{\mathbb{R}^2} p_i \left(\sum_{k=1}^{+\infty} \Theta_k \right)_j dp = -\sum_{k=1}^{+\infty} \int_{\mathbb{R}^2} \frac{(\Theta_k)_j Q_B(\Theta_i)_k}{\mathcal{M}_k}\, dp = -\langle \Theta_j, Q_B(\Theta_i)\rangle_{\mathcal{M}}.$$

The selfadjointness of Q_B implies the symmetry of $\mathbb{D}$. For $X \in \mathbb{R}^2$, we set $f_X = X_1\Theta_1 + X_2\Theta_2$,

$$\langle \mathbb{D}X, X\rangle_{\mathcal{M}} = \sum_{1\leq i,j\leq 2} \mathbb{D}_{i,j} X_i X_j = -\langle Q_B(f_X), f_X\rangle_{\mathcal{M}}.$$

Since $\Theta \in (Ker\, Q_B)^\perp$, we have $f_X \in (Ker\, Q)^\perp$. Using (18), we get :

$$\langle \mathbb{D}X, X\rangle_{\mathcal{M}} \geq \alpha_1 \|f_X\|^2_{\mathcal{M}}.$$

We conclude by showing that $X \mapsto \|f_X\|_{\mathcal{M}}$ is a norm on $\mathbb{R}^2$. Actually, the linearity of Q_B gives

$$\sum_{i=1}^{2} X_i \Theta_i = 0 \Rightarrow \sum_{i=1}^{2} X_i Q_B(\Theta_i)_k = 0, \forall\, k \geq 1.$$

This implies that $\sum_i X_i p_i \mathcal{M}_k = 0$, $\forall\, k \geq 1$. Thus $X = 0$. □

Remark 3.9 Particular case when α is a constant
Let us assume that for all k, k', p, p', $\alpha(k, p, k', p') = 1/\tau$, where τ is a relaxation time independent of p, which might depend on some parameters like time t and position x. Then, $\mathbb{D}$ is equal to :

$$\mathbb{D} = \sum_{k=1}^{+\infty} \int_{\mathbb{R}^2} \tau \mathcal{M}_k \frac{p}{m^*} \otimes \frac{p}{m^*}\, dp = \tau Id. \tag{24}$$

3.2 Asymptotic expansion for the diffusive limit

We will show in this section the formal diffusive limit of the Boltzmann equation (11) as $\eta \to 0$, using a Hilbert expansion. First, we recall an existence result for our problem which is a direct corollary of well-known existence results on the Boltzmann equation (see for instance [30], [31]).

Theorem 3.10 *For fixed $\eta > 0$, under Assumptions 3.1, 3.2 and 3.3, the Boltzmann boundary value problem* (11)–(15) *admits a unique weak solution $f^\eta \in L^\infty_{loc}(\mathbb{R}^+, \ell^1(L^1(\mathbb{R}^2 \times \mathbb{R}^2)))$ with $f^\eta \geq 0$.*

Proposition 3.11 *Under Assumptions 3.1, 3.2 and 3.3, if the solution f^η in Theorem 3.10 admits a Hilbert expansion with respect to η, $f^\eta = f^0 + \eta f^1 + \ldots$, then $f^0 = N_s \mathcal{M}$ and N_s is the solution of the drift-diffusion equation*

$$\partial_t N_s - \text{div}_x(\mathbb{D}(\nabla_x N_s + \beta N_s \nabla_x U_s)) = 0, \tag{25}$$

where $\mathbb{D}$ is given in (23) *and U_s is defined by*

$$U_s = -k_B T_L \log \mathcal{Z}. \tag{26}$$

Proof. Formally, inserting the expansion into (11) and neglecting higher order terms, we have :

$$Q_B(f^0)_k + \eta Q_B(f^1)_k + O(\eta^2) = \eta\left(\frac{p}{m^*} \cdot \nabla_x f^0_k - \nabla_x \epsilon_k \cdot \nabla_p f^0_k\right) + O(\eta^2).$$

By identification with respect to powers of η, we get $f^0 \in Ker\, Q_B$. Thus, Proposition 3.5 (iii) gives:

$$f_k^0 = N_s \mathcal{M}_k \ , \quad \forall k \geq 1. \tag{27}$$

Moreover, f^1 is solution of the integral equation

$$Q_B(f^1)_k = H_k, \tag{28}$$

where we define

$$H_k = \frac{p}{m^*} \cdot \nabla_x f_k^0 - \nabla_x \epsilon_k \cdot \nabla_p f_k^0.$$

By Corollary 3.7, f^1 exists iff

$$H \in (Ker Q_B)^{\perp}. \tag{29}$$

Differentiating $\mathcal{M}_k$ with respect to x and p, we obtain

$$\nabla_x \mathcal{M}_k = -\beta \mathcal{M}_k \nabla_x \epsilon_k + \beta \mathcal{M}_k \nabla_x U_s,$$

with U_s defined in (26), and

$$\nabla_p \mathcal{M}_k = -\frac{\beta p}{m^*} \mathcal{M}_k.$$

Therefore, from (27) it follows

$$H_k = \mathcal{M}_k \frac{p}{m^*} \cdot (\nabla_x N_s + \beta N_s \nabla_x U_s).$$

Since $p\mathcal{M}_k$ is an odd function, we have $\int p\mathcal{M}_k \, dp = 0$, so that (29) holds. We choose $\Theta \in (L^2_{\mathcal{M}})^2$ as in (22). Thus,

$$f^1 = -\Theta \cdot (\nabla_x N_s + \beta N_s \nabla_x U_s). \tag{30}$$

We integrate (11) with respect to p and sum over k. By observing that $\int \nabla_p f_k^\eta \, dp = 0$, and by using Proposition 3.5 (i), we obtain

$$\partial_t \int_{\mathbb{R}^2} \sum_k f_k^\eta \, dp + \frac{1}{\eta} \int_{\mathbb{R}^2} \sum_k \frac{p}{m^*} \cdot \nabla_x f_k^\eta \, dp = 0.$$

Moreover, the second term can be written as follows

$$\begin{aligned} \frac{1}{\eta} \int \frac{p}{m^*} \cdot \nabla_x f_k^\eta \, dp &= \frac{1}{\eta} \int \frac{p}{m^*} \cdot \nabla_x (N_s \mathcal{M}_k) \, dp + \int \frac{p}{m^*} \cdot \nabla_x f_k^1 \, dp + O(\eta) \\ &= -\mathrm{div}_{\, x} \int (\Theta_k \otimes \frac{p}{m^*})(\nabla_x N_s + \beta N_s \nabla_x U_s) \, dp + O(\eta), \end{aligned}$$

thanks to (30). By assuming that we can pass to the limit, we find the *drift-diffusion* equation :

$$\partial_t N_s - \mathrm{div}_{\, x}(\mathbb{D} \cdot (\nabla_x N_s + \beta N_s \nabla_x U_s)) = 0,$$

where the operator $\mathbb{D}$ is defined in (23). $\square$

3.3 The 3 valley case

Our physical devices of interest are nanoscale Double-Gate-MOSFETs of silicon structure. Due to effective mass anisotropy in silicon valleys, we introduce the transverse effective mass m_t^* and the longitudinal one m_ℓ^*. Then three different electron configurations appear in the band structure, counted twice, due to the symmetry of each valley (see Figure 1): (m_t^*, m_t^*, m_ℓ^*), (m_t^*, m_ℓ^*, m_t^*) and (m_ℓ^*, m_t^*, m_t^*). In the following, we will consider the generic configuration (m_x^*, m_y^*, m_z^*), where m_x^* (m_y^* and m_z^*, respectively) corresponds to the effective mass in the x direction (y and z direction, respectively). Notice a slight change of notation from the previous sections, where the transport directions are simply denoted by x.

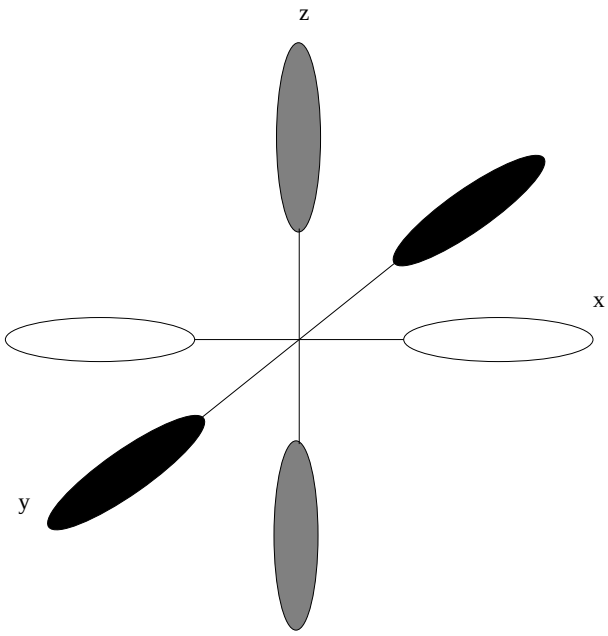

Figure 1: Surface of constant energy in the first conduction band of silicon (six ellipsoids and three different configurations for the electrons due to the symmetry properties).

In this section, we explain briefly the modification of the system when we take into account the three different configurations.

The distribution function of the kth subband and the ith valley, denoted by f_k^i $(i = 1, 2, 3)$, satisfies the following Boltzmann equation :

$$\eta \partial_t f_k^{i,\eta} + \frac{p_x}{m_x^*} \partial_x f_k^{i,\eta} + \frac{p_y}{m_y^*} \partial_y f_k^{i,\eta} - \partial_x \epsilon_k^i \partial_{p_x} f_k^{i,\eta} - \partial_y \epsilon_k^i \partial_{p_y} f_k^{i,\eta} = \frac{1}{\eta} Q_B(f^\eta)_k^i, \tag{31}$$

with

$$Q_B(f)_k^i = \sum_{k',i'} \int_{\mathbb{R}^2} \alpha_{k,k'}^{i,i'}(p,p') (f_{k'}^{i'}(p') \mathcal{M}_k^i(p) - f_k^i(p) \mathcal{M}_{k'}^{i'}(p'))\, dp'.$$

This collision operator takes into account intravalley and inter-valley collisions. Of course, all the properties stated in Proposition 3.5 still hold. The normalized Maxwellian is now defined by

$$\mathcal{M}_k^i(p) = \frac{\exp\left(-\beta(\frac{p_x^2}{2m_x^*} + \frac{p_y^2}{2m_y^*} + \epsilon_k^i)\right)}{\widetilde{\mathcal{Z}}}, \tag{32}$$

where the normalization coefficient is defined by

$$\widetilde{\mathcal{Z}} = \sum_{k,i} \int_{\mathbb{R}^2} e^{-\beta(\frac{p_x^2}{2m_x^*} + \frac{p_y^2}{2m_y^*} + \epsilon_k^i)}\, dp. \tag{33}$$

Proposition 3.12 *Let $f^\eta \in L^\infty([0,T], L^2_{\mathcal{M}})$ be a solution of the three valley Boltzmann equation* (31) *coupled with the subband problem* (35)-(37)*. Then, formally, as $\eta \to 0$ the solution f^η converges towards $N_s\mathcal{M}_k$, where N_s is the solution of the drift-diffusion equation* (34) *coupled with the Schödinger-Poisson system* (35)-(37) *:*

$$\partial_t N_s + \text{div}\,(\mathbb{D}(\nabla N_s + \beta N_s \nabla U_s)) = 0, \tag{34}$$

$$-\frac{1}{2}\frac{d}{dz}\left(\frac{1}{m_t^*}\frac{d}{dz}\chi_k^t\right) + U\chi_k^t = \epsilon_k^t\chi_k^t, \quad \chi_k^t \in H^1(0,1), \int_0^\ell \chi_k^t\chi_{k'}^t\, dz = \delta_{kk'}, \tag{35}$$

$$-\frac{1}{2}\frac{d}{dz}\left(\frac{1}{m_\ell^*}\frac{d}{dz}\chi_k^\ell\right) + U\chi_k^\ell = \epsilon_k^\ell\chi_k^\ell, \quad \chi_k^\ell \in H^1(0,1), \int_0^\ell \chi_k^\ell\chi_{k'}^\ell\, dz = \delta_{kk'}, \tag{36}$$

$$\text{div}_{\,x,z}(\varepsilon_R(x,z)\nabla_{x,z}V) = \frac{e}{\varepsilon_0}(N - N_D), \tag{37}$$

where

$$U = -eV\ ; \qquad N = \frac{N_s}{\mathcal{Z}}\sum_{k=1}^{+\infty}\left(2e^{-\beta\epsilon_k^\ell}|\chi_k^\ell|^2 + 4\sqrt{\frac{m_\ell^*}{m_t^*}}e^{-\beta\epsilon_k^t}|\chi_k^t|^2\right), \tag{38}$$

$$U_s = -k_BT_L\log\mathcal{Z}\ ; \qquad \mathcal{Z} = 2\sum_{k=1}^{+\infty}e^{-\beta\epsilon_k^\ell} + 4\sqrt{\frac{m_\ell^*}{m_t^*}}\sum_{k=1}^{+\infty}e^{-\beta\epsilon_k^t}. \tag{39}$$

$\mathbb{D}$ is a symmetric coercive matrix which will be determined in the proof (see (40)*), $\beta = 1/k_BT_L$. Moreover, ϵ_R, ϵ_0, e, N_D in* (37) *are defined as in Section 2.*

Proof. As before, we assume that f^η admits a Hilbert expansion of the form: $f^\eta = f^0 + \eta f^1 + ...$ Then, by identification with respect to powers of η, we obtain

$$Q_B(f^0)_k^i = 0,$$

that implies $f_k^{0,i} = N_s\mathcal{M}_k^i$, and

$$Q_B(f^1)_k^i = \frac{p_x}{m_x^*}\partial_x(N_s\mathcal{M}_k^i) + \frac{p_y}{m_y^*}\partial_y(N_s\mathcal{M}_k^i) - \partial_x\epsilon_k^i\partial_{p_x}f_k^{0,i} - \partial_y\epsilon_k^i\partial_{p_y}f_k^{0,i}.$$

We can prove in the same manner as in Proposition 3.8 that there exists a function $\Theta^i \in L^2_{\mathcal{M}^i}$ such that $Q_B(\Theta_x)^i_k = -\frac{p_x}{m^*_x}\mathcal{M}^i_k$ and $Q_B(\Theta_y)^i_k = -\frac{p_y}{m^*_y}\mathcal{M}^i_k$. Therefore,

$$f^{1,i} = -(\nabla_{x,y} N_s + \beta N_s \nabla_{x,y}(-k_B T_L \log \widetilde{\mathcal{Z}}))\Theta^i_k.$$

We define the diffusion matrix (which is symmetric and coercive) as

$$\mathbb{D} = \sum_{k,i} \int_{\mathbb{R}^2} \Theta^i_k \otimes \frac{p}{m}\, dp, \tag{40}$$

where $\frac{p}{m} = (\frac{p_x}{m^*_x}, \frac{p_y}{m^*_y})$. Integrating equation (31) and passing formally to the limit $\eta \to 0$, we get :

$$\partial_t N_s + \text{div}_{x,y}(\mathbb{D}(\nabla_{x,y} N_s + \beta N_s \nabla_{x,y}(-k_B T_L \log \widetilde{\mathcal{Z}}))) = 0. \tag{41}$$

Moreover,

$$\widetilde{\mathcal{Z}} = \frac{2\pi}{\beta} \sum_{k,i} \sqrt{m^*_x m^*_y}\, e^{-\beta \epsilon^i_k}.$$

Since the possible configurations for silicon are the three following configurations (counted twice for symmetry reasons) (m^*_t, m^*_t, m^*_ℓ), (m^*_t, m^*_ℓ, m^*_t) and (m^*_ℓ, m^*_t, m^*_t), we have

$$\widetilde{\mathcal{Z}} = \frac{2\pi}{\beta}(2m^*_t \sum_k e^{-\beta\epsilon^1_k} + 2\sqrt{m^*_t m^*_\ell} \sum_k e^{-\beta\epsilon^2_k} + 2\sqrt{m^*_t m^*_\ell} \sum_k e^{-\beta\epsilon^3_k}).$$

The eigenenergies ϵ^i_k of the kth subband and the ith valley are the eigenvalues of the Hamiltonian in the z-direction. Thus, these quantities only depends on the effective mass on the z-direction :

$$-\frac{1}{2}\frac{d}{dz}\left(\frac{1}{m^*_z}\frac{d}{dz}\chi^i_k\right) + U\chi^i_k = \epsilon^i_k \chi^i_k.$$

The density of charge carriers for the whole system, which enters Poisson equation (37), is given by

$$N = \sum_{k,i} \int_{\mathbb{R}^2} N_s \mathcal{M}^i_k(p) |\chi^i_k|^2\, dp.$$

We have two configurations in which $m^*_z = m^*_t$, thus the eigensystem is $(\epsilon^t_k, \chi^t_k)_{k\geq 1}$ for four ellipsoids. And there is one configuration where $m^*_z = m^*_\ell$, the eigensystem is then $(\epsilon^\ell_k, \chi^\ell_k)_{k\geq 1}$ for two ellipsoids. Thus we have,

$$\widetilde{\mathcal{Z}} = \frac{2\pi}{\beta} m^*_t \left(2\sum_{k=1}^{+\infty} e^{-\beta\epsilon^\ell_k} + 4\sqrt{\frac{m^*_\ell}{m^*_t}} \sum_{k=1}^{+\infty} e^{-\beta\epsilon^t_k}\right).$$

For simplicity of notation, we prefer to use $\mathcal{Z}$ as defined in (39) to obtain

$$N = \frac{N_s}{\mathcal{Z}} \sum_{k=1}^{+\infty} \left(2e^{-\beta\epsilon^\ell_k}|\chi^\ell_k|^2 + 4\sqrt{\frac{m^*_\ell}{m^*_t}} e^{-\beta\epsilon^t_k}|\chi^t_k|^2\right).$$

Notice that $\nabla_{x,y}(\log \mathcal{Z}) = \nabla_{x,y}(\log \widetilde{\mathcal{Z}})$, so that the drift-diffusion equation (41) coincides with (34).

□

4 Numerical implementation

4.1 The modeled device

In this work we are interested in a nanoscale Double-Gate MOSFET (Metal Oxide Semiconductor Field Effect Transistor). The device consists of a silicon film, characterized by two highly doped regions near the Ohmic contacts (denoted by source and drain) and an active region, called channel, with lower doping. The silicon film is sandwiched between two thin layers of silicon dioxide SiO_2, each of them with a gate contact.

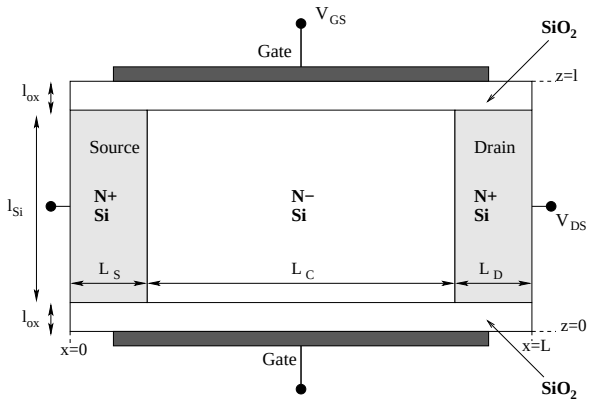

Figure 2: Schematic representation of the modeled device.

We assume invariance in the y direction (infinite boundary conditions), so that the problem is studied in a (x, z)-domain. The device occupies a region of a 2D domain denoted by Ω=$[0, L] \times [0, \ell]$. A schematic representation of the device is shown in Figure 2.

For the sake of completeness, we recall the stationary drift–diffusion Schrödinger–Poisson system which is used for the simulation, taking into account the presence of the oxide and the anisotropy of silicon. As before, we will use the notation $\beta = 1/k_B T_L$.

Find $N_s(x)$, $(\epsilon_k^t(x), \chi_k^t(x, z))$, $(\epsilon_k^\ell(x), \chi_k^\ell(x, z))$, for $k \geq 1$, and $V(x, z)$ such that

$$\frac{d}{dx}\left(\mathbb{D}\left(\frac{d}{dx}N_s + \beta N_s \frac{d}{dx}U_s\right)\right) = 0 \qquad \text{in } (0, L), \tag{42}$$

$$\begin{cases} -\dfrac{\hbar^2}{2}\dfrac{d}{dz}\left(\dfrac{1}{m_t^*(z)}\dfrac{d}{dz}\chi_k^t\right) + (U+U_c)\chi_k^t = \epsilon_k^t\chi_k^t. \\ \chi_k^t(x,\cdot) \in H_0^1(0,\ell), \quad \displaystyle\int_0^\ell \chi_k^t\,\chi_{k'}^t\,dz = \delta_{kk'}\,, \end{cases} \tag{43}$$

$$\begin{cases} -\dfrac{\hbar^2}{2}\dfrac{d}{dz}\left(\dfrac{1}{m_\ell^*(z)}\dfrac{d}{dz}\chi_k^\ell\right) + (U+U_c)\chi_k^\ell = \epsilon_k^l\chi_k^\ell. \\ \chi_k^\ell(x,\cdot) \in H_0^1(0,\ell), \quad \displaystyle\int_0^\ell \chi_k^\ell\,\chi_{k'}^\ell\,dz = \delta_{kk'}\,, \end{cases} \tag{44}$$

$$\text{div}_{\,x,z}(\varepsilon_R(x,z)\nabla_{x,z}V) = \frac{e}{\varepsilon_0}(N-N_D) \qquad \text{in } \Omega, \tag{45}$$

where

$$U = -eV\ ; \qquad N = \frac{N_s}{\mathcal{Z}}\sum_{k=1}^{+\infty}\left(2e^{-\beta\epsilon_k^\ell}|\chi_k^\ell|^2 + 4\sqrt{\frac{m_\ell^*}{m_t^*}}e^{-\beta\epsilon_k^t}|\chi_k^t|^2\right), \tag{46}$$

$$U_s = -k_BT_L\log\mathcal{Z}\ ; \qquad \mathcal{Z} = 2\sum_{k=1}^{+\infty}e^{-\beta\epsilon_k^\ell} + 4\sqrt{\frac{m_\ell^*}{m_t^*}}\sum_{k=1}^{+\infty}e^{-\beta\epsilon_k^t}. \tag{47}$$

In (43)-(44) U_c is a given potential barrier between the silicon and the oxide. Moreover, the diffusion coefficient $\mathbb{D}$ in (42), and ϵ_R, ϵ_0, e, N_D in (45) are defined as in Section 2. Finally, m_t^* and m_ℓ^* denote effective masses: in silicon they are different in the transverse (m_t^*) and in the longitudinal direction (m_ℓ^*), while in the oxide they take the same value. The system is then supplemented by boundary conditions. At the ohmic source, drain, and gate contacts (denoted by Γ_S, Γ_D, and Γ_G, respectively) Dirichlet boundary conditions are imposed. The remaining part of the boundary (denoted by Γ_N) is considered insulated, and homogeneous Neumann boundary conditions are imposed. More precisely, due to the high doping, the drain and the source contacts can be considered as small electron reservoirs in which we assume that the potential does not depend on the transport direction. Therefore, the surface density N_s at the vicinity of the drain and source contacts is assumed to be constant and is then equal to $N^+ \times \ell_{Si}$.

Moreover, the electrostatic potential V equals the sum of the applied voltage and the potential at thermal equilibrium, that we denote by $V_b(x_c,z)$, with $x_c = 0$ or $x_c = L$. In order to find $V_b(x_c,z)$ the following 1D Schrödinger-Poisson system must be solved on the vertical edge $x = x_c$

$$\begin{cases} -\dfrac{\hbar^2}{2}\dfrac{d}{dz}\left(\dfrac{1}{m_t^*(z)}\dfrac{d}{dz}\chi_k^t\right) + (U_b+U_c)\chi_k^t = \epsilon_k^t\chi_k^t. \\ \chi_k^t(x_c,\cdot) \in H_0^1(0,\ell), \quad \displaystyle\int_0^\ell \chi_k^t\,\chi_{k'}^t\,dz = \delta_{kk'}\,, \end{cases} \tag{48}$$

$$\begin{cases} -\dfrac{\hbar^2}{2}\dfrac{d}{dz}\left(\dfrac{1}{m_\ell^*(z)}\dfrac{d}{dz}\chi_k^\ell\right) + (U_b+U_c)\chi_k^\ell = \epsilon_k^l\chi_k^\ell. \\ \chi_k^\ell(x_c,\cdot) \in H_0^1(0,\ell), \quad \displaystyle\int_0^\ell \chi_k^\ell\,\chi_{k'}^\ell\,dz = \delta_{kk'}\,, \end{cases} \tag{49}$$

$$\frac{d}{dz}\left(\varepsilon_R(x_c,z)\frac{d}{dz}V_b\right)=\frac{e}{\varepsilon_0}(N-N_D),\quad V_b=0\quad\text{at } z=0 \text{ and } z=\ell, \tag{50}$$

where

$$U_b=-eV_b,\qquad N(x_c,z)=\frac{N_s(x_c)}{\mathcal{Z}(x_c)}\sum_{k=1}^{+\infty}\left(2e^{-\beta\epsilon_k^\ell}|\chi_k^\ell|^2+4\sqrt{\frac{m_\ell^*}{m_t^*}}e^{-\beta\epsilon_k^t}|\chi_k^t|^2\right),$$

$$\mathcal{Z}(x_c)=2\sum_{k=1}^{+\infty}e^{-\beta\epsilon_k^\ell}+4\sqrt{\frac{m_\ell^*}{m_t^*}}\sum_{k=1}^{+\infty}e^{-\beta\epsilon_k^t}.$$

Summarizing, the boundary conditions for system (42)– (45) are

$$N_s=N^+\times\ell_{S_i}\quad\text{at } x=0 \text{ and } x=L, \tag{51}$$

$$V(z)=V_b(0,z)\quad\text{on }\Gamma_S,\qquad V(z)=V_b(L,z)+V_{DS}\quad\text{on }\Gamma_D, \tag{52}$$

$$V(x)=V_{Gate}\quad\text{on }\Gamma_G, \tag{53}$$

$$\frac{\partial V}{\partial n}=0\quad\text{on }\Gamma_N. \tag{54}$$

4.2 Iterative procedure

We introduce a partition of $[0,L]$ with nodes x_i, $i=1,\cdots,N_x$, and a partition of $[0,\ell]$ with nodes z_j, $j=1,\cdots,N_z$. Then, we mesh the domain $[0,L]\times[0,\ell]$ with rectangular triangles using the nodes (x_i,z_j) previously defined. The Schrödinger equations and the Poisson equation are discretized with conforming P^1 finite elements, while for the 1D drift-diffusion equation the Scharfetter–Gummel scheme is used (see [32],[33]). From now on, when referring to equations and formulas (42)–(54) we intend their discretized counterpart.

The first step for initializing the procedure is the computation of V_b on the source and drain contacts. To this aim a Gummel iteration method, described at the end of this section, is used to solve the 1D Schrödinger-Poisson system.

Secondly, we consider the whole system for zero applied source-drain voltage. Equation (42) does not need to be solve in this case. Actually, the Slotboom variable $u=N_s/\mathcal{Z}$, solution of the 1D equation (10), is constant. It is then sufficient to evaluate it on the boundary (for $x=0$ for instance), where N_s is prescribed. It remains to calculate a 2D Schrödinger-Poisson system, with boundary conditions (52) –(54) and $V_{DS}=0$.

Finally, we consider the resolution of the drift-diffusion-Schrödinger-Poisson system when a drain-source voltage V_{DS} is applied. We start from the previously obtained potential and increment the voltage by steps of $0.02V$.

The iterative procedure for the solution of one drift–diffusion–Schrödinger–Poisson system consists of an iteration on the electrostatic potential and it is summarized in the following steps.

1. For a given potential V_{old} in the whole domain Ω we solve the eigenvalue problems (43)–(44) on each slice of the device ($x = x_i, i = 1, \cdots, N_x$) by diagonalization of the Hamiltonian. Thus, we obtain N_x sets of eigenfunctions $\{\chi_k^t(x_i, z)\}_{i=1,\cdots,N_x}$ and eigenvalues $\{\epsilon_k^t\}$, and N_x sets of eigenfunctions $\{\chi_k^\ell(x_i, z)\}_{i=1,\cdots,N_x}$ and eigenvalues $\{\epsilon_k^\ell\}$.

2. Next, we compute the effective energy U_s from (47). We are then able to solve the 1D stationary drift-diffusion equation (42) with Dirichlet boundary conditions (51).

3. We have then all the ingredients to compute the density N thanks to the expression (46).

4. The Poisson equation is solved in the 2D domain using boundary conditions (52)–(54). The system is solved using the preconditioned conjugate gradient method. A new potential V_{new} is then obtained.

5. We repeat the four previous steps until the difference $\|V_{new} - V_{old}\|_{L^\infty}$ is sufficiently small.

We conclude the description of the iteration procedure with few remarks on implementation aspects.

- The solution of the highly non–linear coupled Schrödinger–Poisson system is the most delicate step in the procedure described above. A simple minded decoupling algorithm fails and a Newton-Raphson method is very expensive. Following the idea of Caussignac et al. [34], we used a Gummel iterative algorithm [35] which amounts to substitute in the procedure the Poisson equation with

$$-\nabla(\varepsilon_R \nabla V_{new}) + \frac{e}{\varepsilon_0} N(x,z) \frac{V_{new}}{V_{ref}} = \frac{e}{\varepsilon_0} \left(N_D - N(x,z) \left(1 - \frac{V_{old}}{V_{ref}} \right) \right),$$

  with $V_{ref} = k_B T_L / e$. This method can be viewed as an approximate Newton method where the Jacobian of the system is replaced by a diagonal matrix, after that information about the strong coupling of the unknowns are incorporated into Poisson equation. This is done by considering an exponential dependence of the electron density N on the potential V. We refer to [5] where this method is used in the simulation of a 2D ballistic Schrödinger–Poisson system.

- When solving the eigenvalue problems it is not necessary to compute all the N_z modes because of the exponential dependence of U_s on the energy levels ϵ_k's (see (47)). Here we used only the first 12 modes.

- The solution of one Schrödinger problem on a slice is independent of the others, therefore, the most costly part of the algorithm is fully and easily parallelizable.

Table 1: Table of the main physical values

Parameter	Value	Length	Value
N^+	$10^{26}m^{-3}$	L_S	$10nm$
N^-	$10^{21}m^{-3}$	L_C	$30nm$
U_c	$3\ eV$	L_D	$10nm$
$\varepsilon_R[Si]$	11.7	ℓ_{ox}	$3nm$
$\varepsilon_R[SiO_2]$	3.9	ℓ_{Si}	4, 5 or $7nm$

5 Numerical results

The silicon region in the Double–Gate MOSFET under consideration consists of source and drain regions, with length L_S and L_D, respectively, which are highly doped with density N^+, and of a channel region, with length L_C which is intrinsic. The total length is $L = L_S + L_C + L_D$. The thickness of the oxide layer is defined by ℓ_{ox} (see Figure 2). The numerical values used in the implementation are reported in Table 1. For such a device geometry short channel effects are acceptable (see e.g. [12]). Denoting by m_e the electron mass, then the transverse and longitudinal effective masses in silicon are $m_t^* = 0.19m_e$ and $m_\ell^* = 0.98m_e$. The effective mass in the oxide is chosen as $0.5m_e$. The lattice is assumed to be at room temperature ($T_L = 300K$).

All the computations in this section are performed with a field dependent mobility (see [8],[9], e.g.) given by

$$\mu(E_s) = \frac{2\mu_0}{1 + \sqrt{1 + (2\mu_0|E_s|/v_{sat})^2}},$$

where $E_s = \frac{d}{dx}U_s$ is the effective electric field, the low field mobility is $\mu_0 = 0.12m^2V^{-1}s^{-1}$ and the saturation velocity is $v_{sat} = 1.1\,10^5ms^{-1}$. The diffusion coefficient in (5) is computed using a generalized Einstein relation $\mathbb{D} = \mu(E)k_BT_L$.

We take $N_x = 50$ points in the transport direction and $N_z = 50$ in the confined direction for all the tests. The first sets of pictures are obtained for $V_{Gate} = 0$ and with $\ell_{Si} = 7nm$. Fig. 3 shows the electron density at the equilibrium state for the one valley case when $m_z^* = m_t^*$ (left) and for the three valley case (right). We notice that, as expected, the configuration of the electron density and thus the confinement are not the same. Figure 4 shows the electron density for a drain-source voltage $V_{DS} = 0.2V$ (left) and $V_{DS} = 0.5V$ (right). Because of this bias, the density does not remain symmetric but the electron concentration is higher in the source region.

In Fig. 5 we present the variation of the first energy levels $\epsilon_k(x)$ in the confined direction z along the transport direction x for the two cases $m_z^* = m_\ell^*$ and $m_z^* = m_t^*$. The results are shown for $V_{DS} = 0V$ (left) and for $V_{DS} = 0.5V$ (right). We recall that the eigenvalues of the Hamiltonian form an increasing sequence of real valued numbers. We notice that the eigenvalues are closer to each other in the configuration $m_z^* = m_\ell^*$ than in the configuration $m_z^* = m_t^*$. This explains why the confinement is

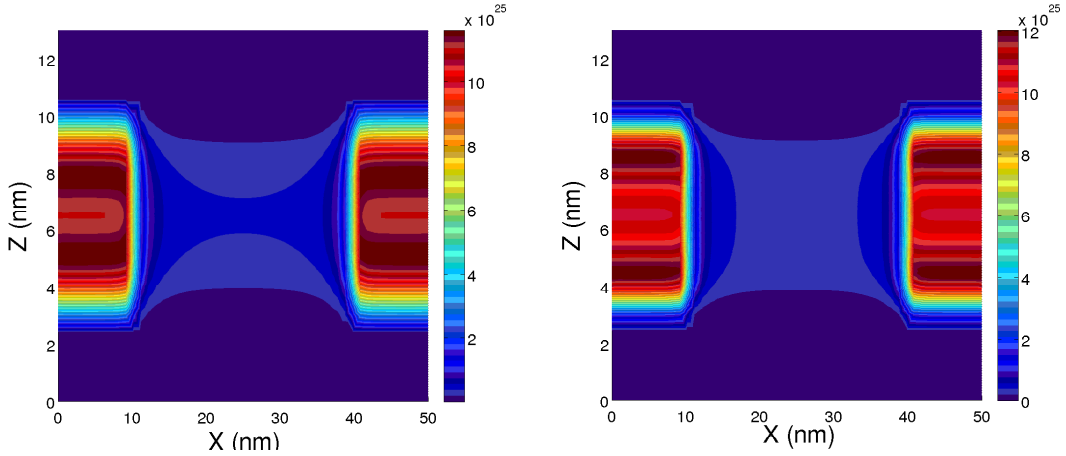

Figure 3: Electron density (in m^{-3}) at the equilibrium state. On the left, we plot the one valley case, while we plot the three valley case on the right.

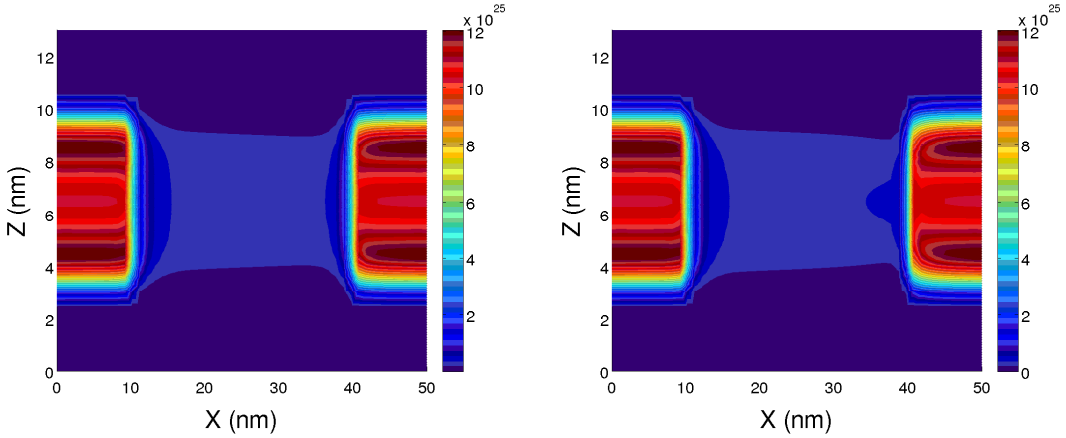

Figure 4: Electron density (in m^{-3}) for an applied Drain-Source potential $V_{DS} = 0.2V$ on the left and $V_{DS} = 0.5V$ on the right.

so different in the two cases. Indeed, if we compute the occupation factor of each state (see Figure 6), we notice that four modes are not negligible when $m_z^* = m_\ell^*$ and only one when $m_z^* = m_t^*$, because of the exponential dependence on ϵ_k. That is the reason why we only consider a finite number of modes in our computation. The choice of 12 computed modes made here is done in order to avoid any loss in accuracy, but in view of these considerations, we could choose less modes for a faster computation. Moreover, in Figure 5 on the right, we observe a shift in the energy levels at the drain contact, which, as expected, is equal to the amplitude of the associated drain voltage.

In Figure 7 we plot the potential energy observed in the device. The energy potential barrier between the source and the channel is visible. The gate voltage V_{Gate} modulates the height of this barrier and thus the number of free electrons in the channel.

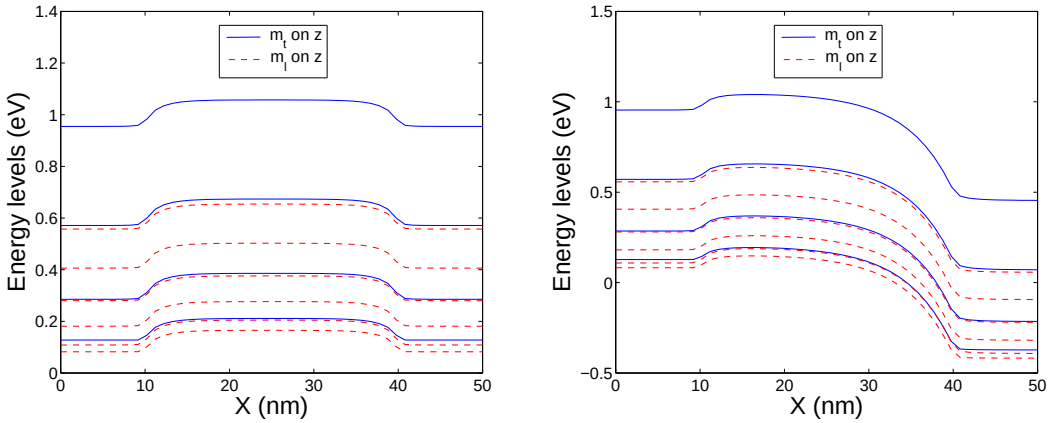

Figure 5: Energy levels $\epsilon_k(x)$ along the x transport direction for the two effective mass configurations in the z direction, at $V_{DS} = 0V$ (on the left) and $V_{DS} = 0.5V$ (on the right).

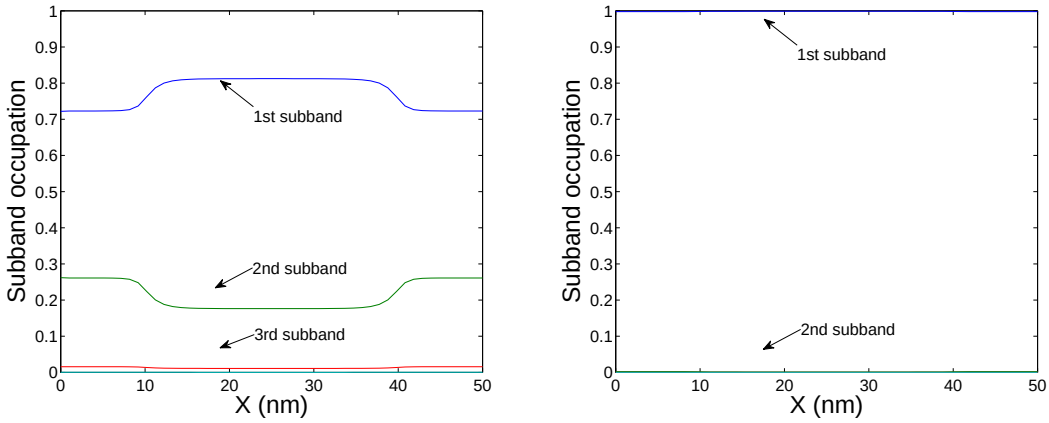

Figure 6: Occupation of each subband in the case $m_z^* = m_\ell^*$ (left) and $m_z^* = m_t^*$ (right). The confinement is much more important in the second case.

The $I-V$ characteristics of the Double-Gate-MOSFET for different gate voltage V_{Gate} are presented in Figure 8. The current is defined by the quantity J in (5). Figure 8 (left) plots drain current versus drain voltage V_{DS} for different gate voltages V_{Gate}, Figure 8 (right) shows drain current versus gate voltage V_{Gate} for different drain voltages, for $\ell_{Si} = 5nm$. Finally, Figure 9 shows the dependence of the current on the silicon thickness ℓ_{Si}. These figures show $I-V$ characteristics similar to that of the conventional MOSFETs with two typical regimes : a ohmic regime for small values of V_{DS} and a quasi-saturation regime. We notice a good agreement with the results presented in [12] where Monte Carlo simulation is used for the same device geometry.

Conclusion A subband decomposition approach has been used to derive a cou-

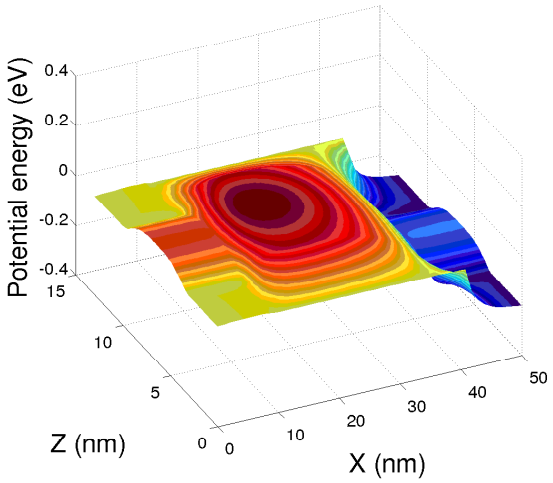

Figure 7: Potential energy for $V_{Gate} = 0V$ and $V_{DS} = 0.2V$.

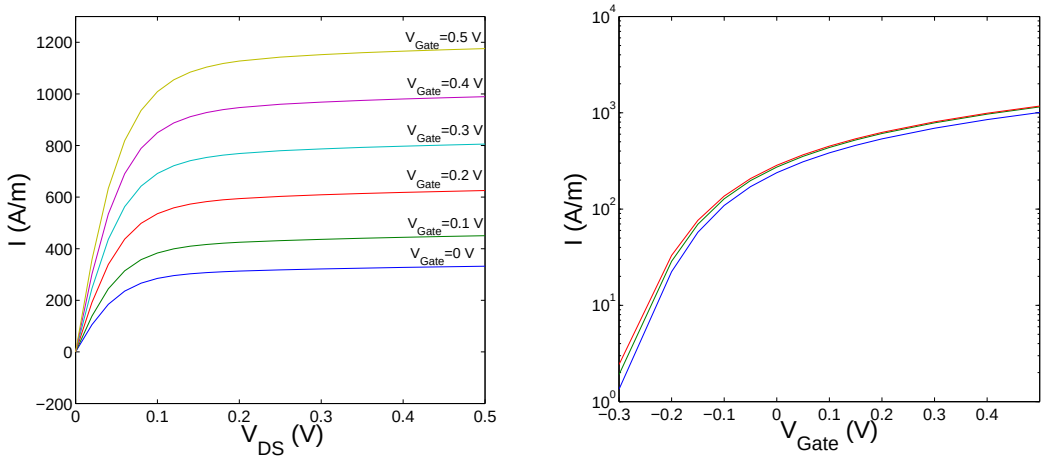

Figure 8: Drain current I in the structure as a function of the drain-source voltage V_{DS} (left) and of the Gate bias V_{Gate} (right) for $V_{DS} = 0.1$ V (blue), 0.3 V (green) and 0.5 V (red) for $\ell_{Si} = 5nm$.

pled quantum–classical system for an electron gas confined in a nanostructure. A single transport equation is obtained with a limiting process in the scaled mean free path from the Boltzmann equations, one for each subband, under a diffusive transport assumption. The model is used to simulate a DG-MOSFET with channel length of $30nm$. The results show that the model provides a good description of the transport in a Double-Gate MOSFET, making it attractive for rapid design computation.

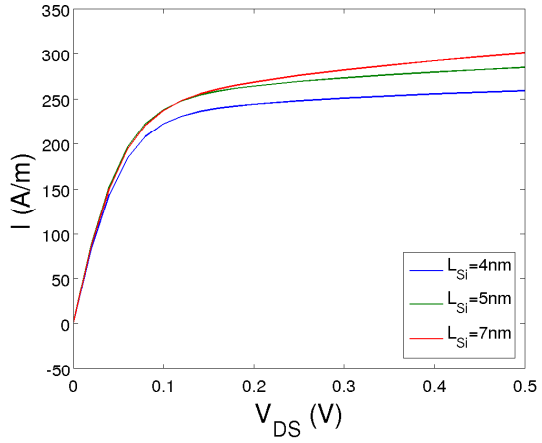

Figure 9: $I-V_{DS}$ characteristics for three different structures which differs only from the Silicon thickness L_{Si} for $V_{Gate} = 0V$.

Acknowledgments. The authors acknowledge partial support from the European IHP Network HPRN-CT-2002-00282"Hyperbolic and kinetic equations: asymptotics, numerics, analysis". The first author acknowledges partial support from INdAM Project "Mathematical modeling and numerical analysis of quantum systems with applications to nanosciences". The authors thank warmly Naoufel Ben Abdallah and Florian Méhats for fruitful discussions. The authors thank the unknown referees for valuable comments and suggestions.

References

[1] G. Bastard, *Wave mechanics applied to semiconductor heterostructures*, Les éditions de Physique, 1996.

[2] J. H. Davies, *The physics of low dimensional semiconductors*, Cambridge Univ. press, 1998.

[3] D. K. Ferry, S. M. Goodnick, *Transport in nanostructures*, Cambridge Univ. Press (1997).

[4] F. Balestra, S. Cristoloveanu, M. Benachir, J. Brini, T. Elewa, *Double gate silicon-on-isulator transistor with volume inversion : A new device with with greatly enhanced performance*, IEEE Electron Device Lett., vol. EDL-8, pp 410–412, Sept 1987.

[5] E. Polizzi, N. Ben Abdallah, *Subband decomposition approach for the simulation of quantum electron transport in nanostructures*, J. Comp. Phys. **202** (2005), 150–180.

[6] N. Ben Abdallah, E. Polizzi, M. Mouis, F. Méhats, *Simulation of 2D quantum transport in ultrashort DG-Mosfets : a fast algorithm using subbands*, Proceedings of the SISPAD conference 2003, IEEE product TH8679-TBR, 267–270 (2003).

[7] M. S. Mock, *Analysis of mathematical models of semiconductor devices*, Advances in Numerical Computation Series 3, Boole Press, 1983.

[8] P. A. Markowich, C. A. Ringhofer, C. Schmeiser, *Semiconductor equations*, Springer-Verlag, Vienna, 1990.

[9] S. Selberherr, *Analysis and simulation of semiconductor devices*, Springer, Wien, 1984.

[10] C. Jungemann, T. Grasser, B. Neinhüs and B. Meinerzhagen, *Failure of moments-based transport models in nanoscale devices near equilibrium*, IEEE Trans Electron Dev 52 (2005) (11), 2404–2408.

[11] M. Nekovee, B.J. Geurts, H.M.J. Boots, M.F.H. Schuurmans, *Failure of extended–moment–equation approaches to describe ballistic transport in submicrometer structures*, Phys. Rev. B, **45** (1992), no. 12, 6643–6651.

[12] G. Baccarani and S. Reggiani, *A compact double-gate MOSFET model comprising quantum-mechanical and nonstatic effects*, IEEE Trans Electron Dev 46 (8) (1999), p. 1656.

[13] C. Negulescu, N. Ben Abdallah, E. Polizzi, M. Mouis, *Simulation Schemes in 2D nanoscale MOSFETs: a WKB based method*, to appear in J. Comp. electronics special issue for the ICWE 10.

[14] M. G. Ancona and G. J. Iafrate, *Quantum correction to the equation of state of an electron gas in a semiconductor*, Phys. Rev. B 40, 7347 (1989).

[15] G. Casssano, C. De Falco, Cl. Giulianetti, R. Sacco, *Numerical simulation of tunneling effects in nanoscale semiconductor devices using quantum corrected drift-diffusion models*, Comput. methods appl. mech. eng. (2006) vol. 195, 19-22, 2193–2208.

[16] G. Curatola, G. Iannaccone, G. Fiori, *Effective Bohm Quantum Potential for device simulators based on drift-diffusion and energy transport*,1-4 september "SISPAD 2004", Munich, Germany, pp. 275-278.

[17] P. Degond, F. Méhats, C. Ringhofer, *Quantum Energy-Transport and Drift-Diffusion models*, J. Stat. Phys. **118** (2005), no. 3-4, 625–665.

[18] S. Gallego, F. Méhats, *Numerical approximation of a quantum drift-diffusion model*, C. R. Acad. Sci. Paris, Ser. I **339** (2004), 519–524.

[19] A. Pirovano, A. Lacaita, A. Spinelli, *Two dimensional Quantum Effects in Nanoscale MOSFETs*, IEEE Trans. Electron. Dev. **49** (2002), no. 1, 25–31.

[20] C. De Falco, E. Gatti, A. L. Lacaita and R. Sacco, *Quantum-corrected drift-diffusion models for transport in semiconductor devices*, J. Comp. Phys. **204** (2005), n.2, 533–561.

[21] A. Jüngel, R. Pinnau, *Convergent semidiscretization of a nonlinear fourth order parabolic system*, Math. Mod. Num. Anal. **37** (2003), 277-289.

[22] F. Nier, *A stationary Schrödinger-Poisson system arising from the modelling of electronic devices*, Forum Math. **2** (1990), no. 5, 489–510.

[23] K. Seeger, *Semiconductor Physics. An Introduction*, 6th edition, Springer, Berlin, 1997.

[24] B. Vinter, C. Weisbuch, *Quantum Semiconductor Structures*, Academic Press, 1991.

[25] F. Golse, F. Poupaud, *Limite fluide des équations de Boltzmann des semiconducteurs pour une statistique de Fermi-Dirac*, Asymptotic Analysis **6** (1992), 135–169.

[26] F. Poupaud, *Diffusion approximation of the linear semiconductor Boltzmann equation : analysis of boundary layers*, Asymptotic Analysis **4** (1991), 293–317.

[27] N. Ben Abdallah, F. Méhats, N. Vauchelet, *Diffusive transport of partially quantized particles : existence uniqueness and long time behaviour*, Proc. Edinb. Math. Soc. (2006) **49**, 513–549.

[28] N. Vauchelet, *Diffusive limit of a kinetic system of partially quantized particles in two dimensions*, submitted.

[29] J. Pöschel, E. Trubowitz, *Inverse spectral theory*, Academic Press, 1987.

[30] N. Ben Abdallah, M.L. Tayeb, *Diffusion approximation for the one dimensionnal Boltzmann-Poisson system* Multiscale Model. Simul. **4** n. 3 (2005), 896–914

[31] F. Bouchut, F. Golse, M. Pulvirenti, *Kinetic equations and asymptotic theory*, Series in Appl. Math., Gauthiers-Villars, 2000.

[32] D.L. Scharfetter, H.K. Gummel, *Large signal analysis of a silicon Read diode oscillator*. IEEE Trans. Electron Devices **ED-16** (1969), 64–77.

[33] F. Brezzi, L.D. Marini, P. Pietra, *Méthodes d'éléments finis mixtes et schéma de Scharfetter-Gummel*, C.R. Acad. Sci. Paris Sér. I, 305 (1987), 599-604.

[34] Ph. Caussignac, B. Zimmermann, R. Ferro, *Finite element approximation of electrostatic potential in one dimensional multilayer structures with quantized electronic charge*, Computing 45, (1990) 251-264.

[35] H.K. Gummel, *A self-consistent iterative scheme for one-dimensional steady state transistor calculations*, IEEE Trans. on Elec Dev., 11 (10) 455, 1964.